EUROPEAN ORGANIZATION FOR NUCLEAR RESEARCH
CERN — AB DEPARTMENT

AB-Note-2006-002 BI

CERN-AB-2006-017 BI

Dead time effect on single photon counting for the longitudinal density monitor of LHC

E. Bravin

CERN AB/BI – Geneva - Switzerland

Abstract

The longitudinal distribution of the protons in the two LHC rings needs to be known with high accuracy. This is required for both: the correct operation of the machine and the understanding of beam dynamics effects that can influence the performances of the collider. One possible way of achieving the required time resolution of *50 ps* and dynamic range of 10^4 is single photons counting of the synchrotron radiation emitted by the beams using avalanche photo diodes (APDs). Although this kind of devices have very short rise times and allow precise time stamping of detected photons, they also have long recovery times (dead time) of the order of hundreds of nanoseconds, much longer than the bunch length of the LHC beams. For this reason it is important to evaluate the masking effect introduced by this dead time, where photons emitted by protons in different longitudinal positions will have different probabilities of being detected.

Geneva, Switzerland
September, 2005

1 Introduction

The knowledge of the longitudinal distribution of the protons in LHC will be very important. The tight constraints on the beam losses require the measurement of the unbunched protons prior to the start of the ramp, where these protons will inevitably be lost.

The debunched protons will also affect beam losses and background at physics flat top where synchrotron radiation renders these particles unstable (the energy lost can not be correctly restored.) The observation of the rates at which protons drift out of the buckets can also help understanding the underlying beam dynamics.

For bunch core measurements a time resolution of the order of *50 ps* is required in order to sample the bunch longitudinal profile with 5 points per sigma (the bunch length is *~250 ps*.) Another important aspect is the dynamic range required from the monitor. In order to study the tails and the diffusion of protons out of the buckets a dynamic range of the order of 10^4 will be required[1].

These two conditions are already quite difficult to achieve, moreover the requirements on the measurement time and update rate makes the measurement more difficult. A possible method consists in counting single synchrotron radiation photons and record their arrival times.

Unfortunately even the best detectors available on the market, with sufficiently low background counts to allow the target dynamic range, have detection times much longer than the bunch length. Avalanche photo diodes (APDs) for example have rise times short enough to allow a correct measurement, at the same time they have long dead times of the order of hundreds of nanoseconds during which the detector work point is restored[2]. This means that once a photon is detected all the subsequently emitted photons, until the detector comes back on line, are discarded.

If the emission probability is not time correlated a simple correction for the real detection time (total time minus the time the detector was blind) can be applied to obtain the absolute rates, and the shape of the profiles (flat) is anyway unperturbed. In our case the emission is strongly time correlated and an analysis of the dead time influence on the absolute rates and shape distortion is required. In this paper the statistics governing the process is deduced and the effect on the measurements estimated using a computer simulation.

2 The longitudinal distribution of the protons in LHC

At nominal operation the LHC will collide *2808* proton bunches on *2808*. The filling pattern is rather complicated due to the injection scheme that involves a chain of several other machines[3][5].

The bunches are initially generated in the CPS complex, here the proton source first, then the 5*0 MeV* LINAC2, the *1.4 GeV* PS BOOSTER and finally the *26 GeV* Proton Synchrotron (PS) will generate batches of *72* bunches separated by *25 ns*. These batches are then sent to the Super Proton Synchrotron (SPS), here three or four PS batches will be accumulated and then accelerated to *450 GeV*. The SPS batches are then sent to the LHC.

In order to allow the SPS injection kickers to fire, the PS batches are spaced by 8 empty bunches (*225 ns*). The same mechanism applies to the LHC where the SPS batches are spaced by *38* empty bunches (975 *ns*) [3][4][5].

There is also another very important filling constraint: the ejection kickers of LHC have a rise time of the order of *1 μs* and therefore an empty region of *3 μs* is foreseen[3]. This region, called the abort gap, is very important for the longitudinal monitoring as it can be used for calibrating the detector. Since at the end of the abort gap there are no effects from the dead time (the dead time is much shorter that this gap so the detector will be surely ready by the end of it), it is possible to use this gap in order to verify the correct functioning of the device and the correction routines.

3 Probability of detection in the general case

Let the case of any continuous proton distribution be considered first. The aim is to calculate the probability that the next photon will be detected at time t for any time $t>0$, assuming that the detector is active at time $t=0$.

In the infinitesimal interval dt around time t the probability $p(t)dt$ of having a photon emitted is given by:

$$p(t)\,dt = \alpha\, n(t)\,dt \tag{1}$$

Where *n(t)* is the protons distribution and α the probability that a proton emits a photon inside the detectors acceptance. The probability that the next photon will be detected at time *t*, *d(t)*, is given by the product of the probability that a photon is emitted at time *t*, *p(t)*, times the probability that no detection happens for any time *t'<t*, *u(t)*. The detection efficiency is consider equal to 100%,

$$d(t) = u(t)\,p(t) \tag{2}$$

Considering that:

$$du = -d(t)\,dt = -u(t)\,p(t)\,dt \tag{3}$$

one can obtain the following expression for u(t):

$$u(t) = e^{-\int_0^t p(\tau)\,d\tau} \tag{4}$$

If the integral is very small it is possible to make a series expansion and rewrite the exponential as:

$$u(t) = 1 - \int_0^t p(\tau)\,d\tau \tag{5}$$

This formula only makes sense if the integral term is much smaller than *1*. *p(t)* can of course not be modified but one can split the integral into the sum of many small intervals.

$$\int_0^t p(\tau)\,d\tau = \sum_{i=0}^{i=N} \int_{\xi_i}^{\xi_{i+1}} p(\tau)\,d\tau \tag{6}$$

Were $\xi_0 = 0$ and $\xi_{N+1} = t$ and using eq.6 together with the properties of the exponential function one can rewrite eq.2 As:

$$u(t) = \prod_{i=0}^{i=N} \left(1 - \int_{\xi_i}^{\xi_{i+1}} p(\tau)\,d\tau \right) \tag{7}$$

If one goes from the continuous to the discrete the time *t* is converted to an index *i* and it is possible to write:

$$p_i = \int_{\delta \cdot i}^{\delta \cdot (i+1)} \alpha\, n(t)\,dt \tag{8}$$

$$\begin{aligned} u_i &= \prod_{j=0}^{i-1} (1 - p_j) \quad && for\ i > 0 \\ u_i &= 1 && for\ i = 0 \end{aligned} \tag{9}$$

Of course the width of the time bin, δ, has to be selected so that the p_i are much smaller than *1* for any value of the index *i*.

In the end the detection probabilities can be written as:

$$\begin{aligned} d_i &= p_i u_i = p_i \prod_{j=0}^{i-1} (1 - p_j) \quad && for\ i > 0 \\ d_i &= p_i && for\ i = 0 \end{aligned} \tag{10}$$

With these formulas it would be already possible to carry out the montecarlo simulation and calculate the expected profiles for any given proton density distribution. In fact some further elaboration of these equations will simplify the montecarlo process.

4 Probability of detection in the LHC case

For the LHC a longitudinal density monitor with an accurate time resolution better than *50 ps* and capable of covering the whole machine length of *89 μs* will be required. This means a profile of $89\ 10^{-6} / 50\ 10^{-12} = 1.8\ 10^{6}$ bins.

One possibility would be to walk through the bins and do a random yes or no decision based on the comparison of a random number and the probability p_i described before. For the LHC case this would require an enormous number of random numbers and computation power. Due to the complex filling scheme it is in fact not possible to simplify the proton density to a small number of bunches (at the limit a single bunch) but the whole machine density distribution has to be used.

Considering a probability of detecting one photon per bunch (very large, as shown later), since one bunch corresponds to *500* bins (*25 ns / 50 ps)* this would mean *500* random decisions per photon count. Considering the number of bunches, *2808*, and the necessary number of counts per bunch to get a reasonable accuracy, *~1000*, the number of steps would already be rather high, $1.4\ 10^{9}$. In a more realistic case of one photon every ten or even hundred bunches the total number of random decisions becomes enormous.

An alternative method consists in calculating the detection time of the next photon by comparing a single random number, *q*, with the integral of the probability *d(t) and* finding the value of *t* for which eq.11 is satisfied.

$$q = \int_0^t d(\tau)\, d\tau \tag{11}$$

In the discrete case this means finding the index *i* for which *q* is the nearest value smaller than D_i, with:

$$\begin{aligned} D_i &= D_{i-1} + d_i = \sum_{k=0}^{i} d_k = \sum_{k=0}^{i} \left[p_k \prod_{j=0}^{k-1} (1 - p_j) \right] && for\ \ i > 0 \\ D_i &= d_i && for\ \ i = 0 \end{aligned} \tag{12}$$

This can be done by calculating the values of the D_i before starting the montecarlo and then applying a lookup routine to the relative monotonic array.

In eq. 12 it has to be noted that the index *k* goes from 0 to *i; D_i* represents thus the value of the integral of *d(t)* at the end of the bin *i*, and this is why one looks for the bin where *q* is the nearest smaller value of D_i such that:

$$\bar{i}: \ \ D_{\bar{i}-1} < q \le D_{\bar{i}} \tag{13}$$

Since *D* is a monotonic array (integral of an always positive function) and seen the definition of *D*, the exact time for which eq. 11 and eq. 13 are satisfied must be contained inside the i^{th} bin.

For simplicity all bunches will be considered to be equal in charge and shape. This allows to simplify the computations since the various *p, u, d* and *D* arrays can be calculated for one bunch only, this is just a convenience and does not reduce the quality of the results.

With these assumptions the probability of having the next count during a whole bunch is calculated and indicated with *S*

$$S = D_N = \sum_{k=0}^{N} \left[p_k \prod_{j=0}^{k-1} (1 - p_j) \right] \tag{14}$$

Where N represents the number of bins per bunch, in the LHC case *N=500*.

The probability of not having a trigger over a whole bunch is also calculated and indicated with α

$$\alpha = u_{N+1} = \prod_{j=0}^{N} (1 - p_j) \tag{15}$$

Where *N+1* is used here since u_N is the probability of not having a trigger before the N^{th} bin while one needs the probability after the N^{th} bin thus the beginning of the $(N+1)^{th}$.

Of course, since either there is or there is not a trigger over a whole bunch it is possible to write:

$$S + \alpha = 1 \tag{16}$$

Another quantity that will be very useful in the simulation is the probability of having the next detection for one of the next *M* bunches. It has been mentioned already that the probability of having the next detection during the next bunch is defined as *S*. The probability of having the detection during the second bunch can be easily written as αS, which corresponds to the probability of not having the detection over the next bunch times the probability of having the detection over the second one.

In general, the probability of having the detection during the M^{th} bunch , P_M (having M start from 0) is given by

$$P_M = \alpha^M S \tag{17}$$

As done before with *d*, it is possible to calculate the integral of *P*, indicated here with *R* and use it to compare with the random number *q*.

$$R_M = \sum_{i=0}^{M} P_M = \sum_{i=0}^{M} \alpha^i S = 1 - \alpha^{M+1} \tag{18}$$

R_M is the value of the integral of *P* at the end of the M^{th} bunch.

In the montecarlo the first step would thus be the generation of a random number $q \in [0,1]$ and then use this value to calculate after how many bunches the next photon will be detected.

$$\bar{M}: \quad R_{\bar{M}-1} < q \le R_{\bar{M}} \tag{19}$$

With some arithmetics the following result is obtained:

$$\bar{M} = floor\left[\frac{\ln(1-q)}{\ln \alpha}\right] \tag{20}$$

Where floor indicates the rounding down to the nearest integer value.

Once decided in which bunch the detection takes place it is possible to use the *D* array to calculate in which bin in the $\bar{M}^{th}$ bunch the detection happens.

In doing so, one must take into consideration the fact that the range for the number q that corresponds to a detection in bunch $\bar{M}$ is given by $R_{\bar{M}} - R_{\bar{M}-1}$, or:

$$\Delta q = R_{\bar{M}} - R_{\bar{M}-1} = (1 - \alpha^{\bar{M}+1}) - (1 - \alpha^{\bar{M}}) = (\alpha^{\bar{M}} - \alpha^{\bar{M}+1}) = \alpha^{\bar{M}} S \tag{21}$$

In the calculations of the array *D* it was obtained that the total probability of having a detection over the bunch was $D_N = S$. The array must then be rescaled so that $D_N = \Delta q$.

An offset equal to $R_{\bar{M}-1}$ should also be added to *D* in order to take into account the missed bunches. A simpler way to proceed is to rescale the number *q* instead of *D* so that:

$$q' = \frac{q - R_{M-1}}{\alpha^M} \tag{22}$$

And use q' in the search inside D.

There is one more aspect to be considered. Until now the beginning of a bunch was always considered as the time *t= 0*. In reality the time *t= 0* can be anywhere inside a bunch. The time *t= 0* means in fact the time at which the detector start to observe again, i.e. when it is turned ON or comes out of the dead time period.

Assuming that the *t= 0* corresponds to the bin $\bar{i}$, the probability that the photon is detected in the current bunch is given by

$$P_0 = \frac{S - D_{\bar{i}}}{u_{\bar{i}}} \tag{23}$$

The explanation for eq. 26 is that in this case the contribution of the bins antecedent $\bar{i}$ has to removed. First $D_{\bar{i}}$ is subtracted from S because it represent the possibility for the photon to be detected for $i \in [0, \bar{i})$ and then a division by $u_{\bar{i}}$ is performed since this term represents the "shadowing" in the detection probability coming from previous detections.

In general, the detection probability for any bunch is given by:

$$\begin{aligned} P_M &= \frac{S - D_{\bar{i}}}{u_{\bar{i}}} \quad for \quad M = 0 \\ P_M &= \frac{S\,\alpha^M}{u_{\bar{i}}} \quad for \quad M > 0 \end{aligned} \tag{24}$$

And the integral (former eq.18) becomes:

$$R_M = \frac{1}{u_{\bar{i}}} \left[\sum_{j=0}^{M} S\,\alpha^j - D_{\bar{i}} \right] = \frac{\left[1 - \alpha^{M+1} - D_{\bar{i}} \right]}{u_{\bar{i}}} \tag{25}$$

Using the new definition of R_M given in eq. 25 the solution of eq. 19 becomes:

$$\bar{M} = floor \left[\frac{\ln\left(1 - D_{\bar{i}} - q\,u_{\bar{i}}\right)}{\ln\left(\alpha\right)} \right] \tag{26}$$

And using eq. 25 eq. 22 can be rewritten as:

$$q' = \frac{(q - R_{M-1})\,u_{\bar{i}}}{\alpha^M} \tag{27}$$

Finally the complete set of tools to carry out the montecarlo simulation is ready.

5 Montecarlo simulation of the LHC case

As already mentioned in the simulation all the bunches are considered to have the same distribution. This allows a simpler calculation since it is sufficient to cope with one *D* histogram and what is more important the *S* and α are the same for all bunches.

The procedure for the montecarlo is quite simple and is illustrated in figure 1. First of all a filling pattern histogram is initialized, this is a *3560* bins histogram in which each element represents one beam bucket. The bins can be either *1* for filled or *0* for empty. In reality the RF system of LHC has a frequency of *400 MHz*, but only every 10^{th} bucket is eligible for filling (*25 ns*), for this simulation it is sufficient to simply consider

the bucket to be *25 ns* long (*40 MHz*.) With this redefinition an empty bucket means a *25 ns* long empty space, or in other words a missing bunch.

Once the filling pattern histogram is ready, the *D* and *u* histograms are calculated using eq. 12 and eq. 9. The parameters *S* and α are also computed using eq. 14 and eq. 15.

At this point the simulation enters a loop over a large number of events. A random number $q \in [0,1]$ is extracted from a uniform distribution. Using as input the position of the previous detection and the dead time, the bunch and bin where the detector becomes operative again is calculated. A jitter in the dead time is also considered to render the simulation more realistic. If this "Up Time" falls inside an empty bucket the bin index is set to zero and the next filled bunch is considered (there can be no detection in an empty bucket.) Using *q* and the values of *D* and *u* corresponding to the "Up Time" bin it is possible to calculate after how many bunches the next photon will be detected, *M*. At this point *q'* (eq. 27) is calculated using *q*, *u* and *M*. This value is then looked up in the *D* histogram using a variable step and direction algorithm. The ai mis to find the index *i* that satisfies eq. 13 (with q replaced by *q'*.) This yields the detection bin, for the detection bunch it is sufficient to simply look up in the filling pattern histogram and skip *M* filled bunches. In reality a more efficient algorithm that uses the integral of the filling pattern histogram is used to speed up the computation but with no other effects on the result.

During these calculations the number of turns (end of turn crossings) is recorded so that the real measurement time can be computed.

Once the "Detection Time" in terms of bunch and bin are calculated, the counter for that particular bin in the longitudinal density histogram is incremented and the next cycle can start until the desired number of events is obtained.

There is a certain number of parameters that need to be introduced in the program, like bunch length, dead time, dead time jitter, probability of having a photon emitted over one bunch and total number of events (counts.)

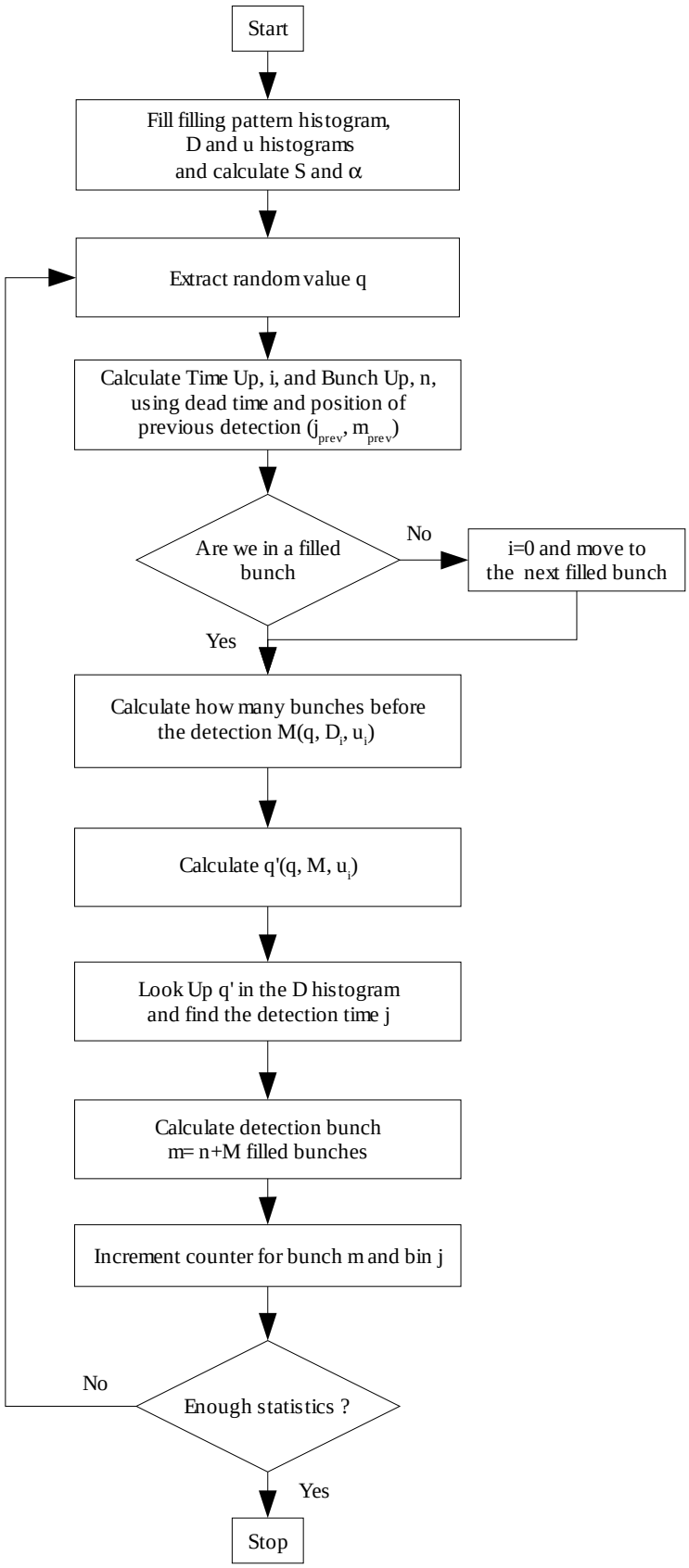

Figure 1: Flow chart of the montecarlo simulation.

6 Alternative computation method

Before proceeding with the results of the montecarlo simulation it might be worth mentioning that there is an alternative method for calculating the probabilities. The complications in the calculations in the method explained above, arises from the time dependency of the emission probability. If one leaves the time domain and use a domain where the emission probability is constant, the calculations will be simpler. In this case the invariant domain is the proton fluence.

The probability that a proton emits a photon is invariant, what is time dependent is the protons density. In this case it is possible to proceed by calculating after how many protons the next detection will happen and then, using the protons distribution, finding the detection bin (time). Eq. 10 is still valid, just need replacing the meaning of the index *i* with the proton number instead of the time bin. Since all the elements p_i are equal eq. 10 can be rewritten as:

$$d_i = (1-p)^{i-1} p = \eta^{i-1} p \tag{28}$$

where η has been used to indicate *(1-p)*. The number of protons can also be considered as a continuous quantity and using *n* to indicate the number of protons gives:

$$d(n) = \eta^n p \tag{29}$$

In this case, using the inversion method, the relation between a uniform *[0,1]* distribution and the distribution of eq. 29 can be easily obtained.

$$n = \frac{\ln\left(1+\frac{q\ln(\eta)}{p}\right)}{\ln(\eta)} = \frac{\ln\left(1+\frac{q\zeta}{p}\right)}{\zeta} \tag{30}$$

where *ln(η)* has been replaced by ζ. In terms of computation work and results, this method is substantially equivalent to the previous one, the complexity of looking up the *D* array is replaced by the complexity of looking up the protons distribution. This method could however be more efficient in the case of a completely arbitrary protons distribution. The mathematical formalism required is also much simpler.

7 Dead Time correction

After the measurement has been simulated and the “measured” longitudinal profile is available, it is possible to reprocess it and try to correct the “measured” values for the effect of the dead time. The correction is quite straight forward. Given any bin *i*, every time that there has been a count in any bin *j* such that $i-\tau < j < i$, τ being the dead time in units of bins, the detector was non operative and therefore could not detect eventually emitted photons. If *N* is the total number of turns over which the measurement spans (number of times a particular bin has passed in front of the detector), only:

$$N'_i = N - \sum_{j=i-\tau}^{i-1} C_j \tag{31}$$

are to be considered, C_j being the content of the counters for the different bins of the profile.

This means that the number of counts in case of no dead time would have been

$$C'_i = C_i \frac{N}{N - \sum_{j=i-\tau}^{i-1} C_j} \tag{32}$$

8 Results of the simulations

The simulations have been carried out assuming the following parameters;

Bunch length(1σ)	*250 ps*
Dead time	*100, 200, 300, 400 ns*
Dead time jitter	*0.1, 1, 2 ns*
Emission probability over 1 bunch	*1% ,10%, 50%*
Number of counts per case (total)	10^8

8.1 Bunch current measurement

Fig. 2 a-b-c show the bunch current plots for the first two PS batches (2x*72* bunches) and for different emission probabilities in the case of a dead time of *200 ns*. Since the dead time considered in this pictures of *200 ns* does not exceed the gap between batches (also *200 ns*) there is no interference from one batch to the next.

The black curve shows the number of emitted photons per bunch and is in fact a constant value. The red curve represents the real counts C_i while the blue curve represents the corrected counts C'_i. It is interesting how the real counts show a damped oscillatory behaviour for large detection probability. The period is slightly different from the dead time due to shadowing effects inside each single bunch. The difference between the emitted and the detected photons is quite large even for small emission probabilities. Eventually this difference becomes negligible for probabilities below *0.1%* not shown in the pictures. It is however quite simple to correct for the dead time shadowing effect as seen before and the difference between the emitted photons and the corrected counts is very small. Only for a 50% probability it is possible to observe substantial errors in the corrected bunch current profile for a reduced number of bunches. For these bunches the problem is that there are too few counts and the statistical fluctuations become important. This effect imposes a limitation on the emission probability linked to the dead time duration.

The maximum suppression (the minimum measured current divided by the real value) can be approximated by

$$\xi = (1-p)^{\tau_D/\tau_b} \tag{33}$$

Where p is the probability of emission over one bunch, τ_D is the dead time and τ_b is the bunch to bunch distance.

And the average of the fraction of detected photons can be approximated by the following formula;

$$\Omega = 1 - \frac{\frac{\tau_D}{\tau_b} p}{1 + \frac{\tau_D}{\tau_b} p} \tag{34}$$

In order to have small differences in the measurement error Ω and $1-\xi$ must not differ too much. In fact, for example, a factor 4 in the counts corresponds to only a factor two in the error, it is therefore not strictly necessary that those two numbers are equal.

Table shows the values of Ω and $1-\xi$ for different cases, including those simulated in Fig. 2. It is clear from this table how, for the large emission probabilities, the difference can be very large (this was already clearly visible in Fig. 2-a.) The optimum lies somewhere between 10% and 30%, depending on the trade off between precision and measuring time.

Fig. 2-*d* shows the distributions of the measurement errors after the correction for the dead time. The measurement error is defined as the difference between the real value and the dead time corrected number of counts divided by the real value. It is clear how for probabilities of 10% or less the measurement error is very small and the distribution is dominated by the statistical fluctuations due to the limited number of events. For

the 50% probability case however there is a clear systematic effect that is caused by the shadowing effect. The distribution in this case is slightly shifted and has tails. The tails correspond to the bunches with a high suppression coefficient (around the 9th bunch of every batch.)

Fig. 3 Shows the bunch profiles for the first 9 bunches of the first PS batch. The different colour curves indicate the real, detected and dead time corrected profiles. The difference between real and corrected is so small that in this scale they are undistinguishable.

p	Ω	$1-\xi$	$\Omega / 1-\xi$	$\sqrt{\frac{\Omega}{1-\xi}}$
50%	20%	0.4%	50	7
30%	29%	5.8%	5	2
20%	38%	17%	2.2	1.5
10%	55%	43%	1.3	1.1
1%	93%	92%	1.0	1.0

Table 1 Approximated average fraction of detected photons, maximum suppression and their ratios for different emission probabilities. τ_D=200 ns, τ_b=25 ns

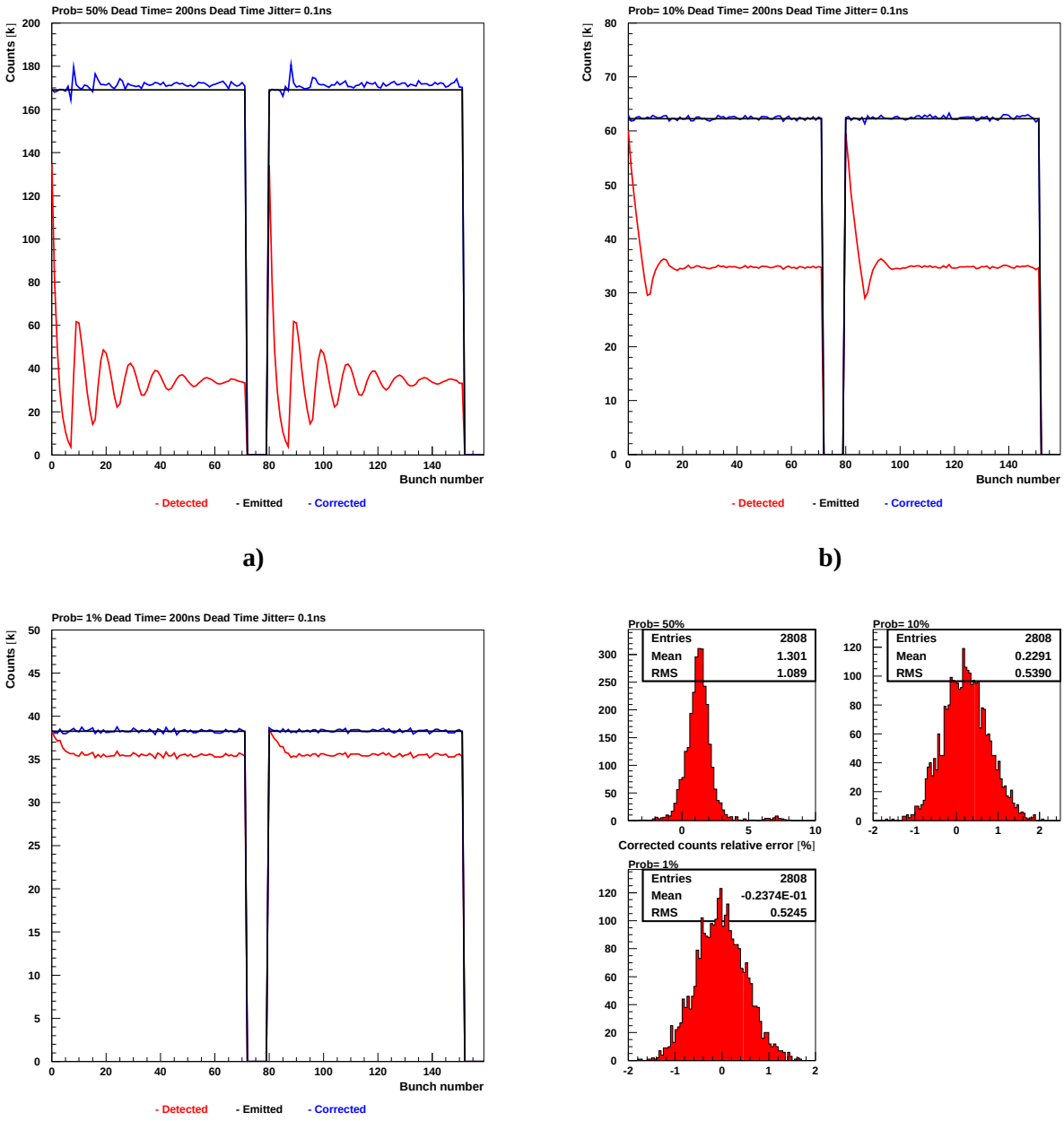

Figure 2: a) b) c) "Measured" bunch current vs. bunch number for different emission probabilities. The emission probability indicated on the plots is the probability of having a photon emitted over a period of 25ns. Only the data relative to the first two PS batches is showed (144 bunches.) The black curve represents the emitted photons, the red curve the detected photons and the blue curve the detected photons after correction for the dead time. d) Shows the histograms of the deviations of the counts after correction for the dead time from the real values (emitted photons), these plots refer to the whole ring.

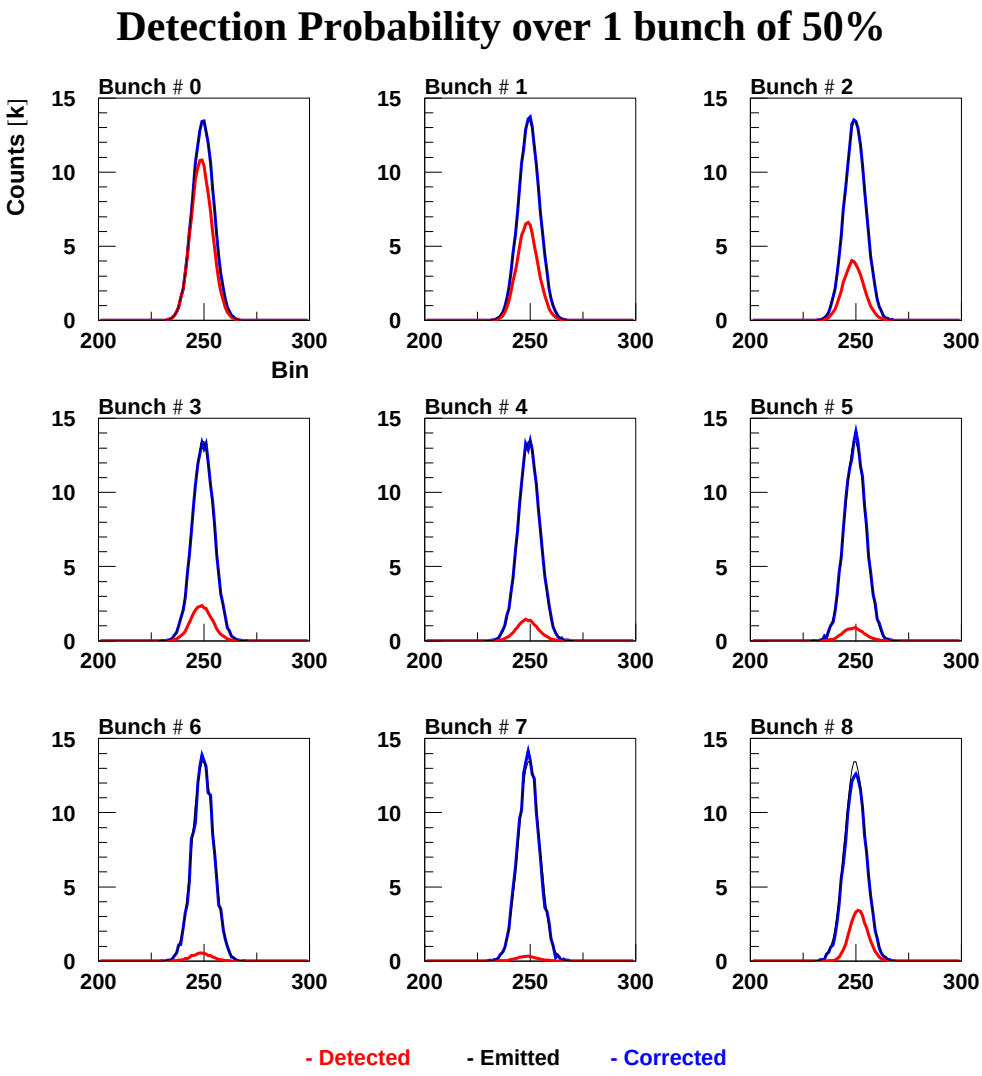

Figure 3 First 9 bunches of the first batch in the case of an emission probability of 50% and dead time of 200ns, dead time jitter is 100ps. The black curve indicates the real bunch, red the detected profile and blue the corrected one.

8.2 Detector performances

In the following pages several plots will be presented for the different cases simulated. The results will be analysed and the most important points highlighted.

8.2.1 Dead Time 100ns and jitter 0.1ns

For each bunch in the ring a Gaussian fit is calculated. The fitted gaussian have three free parameters; centre, sigma and amplitude. The plots in Fig.5 show the distributions of the deviations of the fitted values from the known real value (input to the simulation.)

It can be observed that there are no systematic effects for the bunch lengths and the widths of the distributions agree with the values expected [6]. In fact the widths are dominated by the limited number of photons per profile (~10^8/2808~350k.) For the centre position and amplitude there could be a small systematic effect for high emission probabilities.

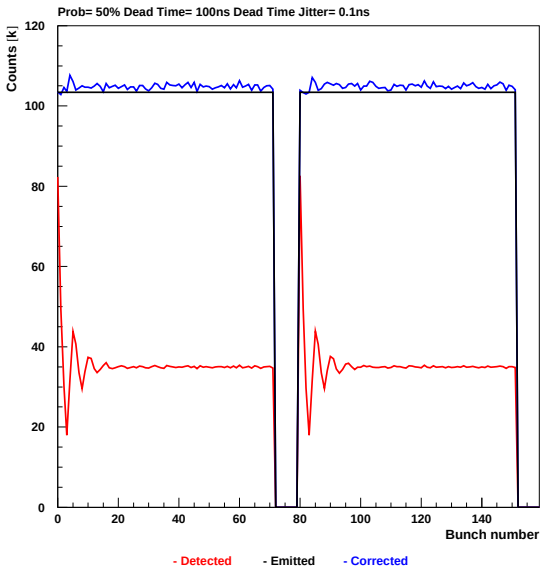

a)

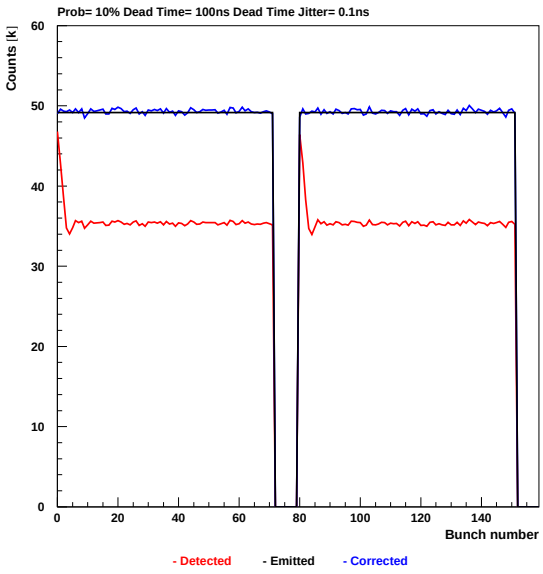

b)

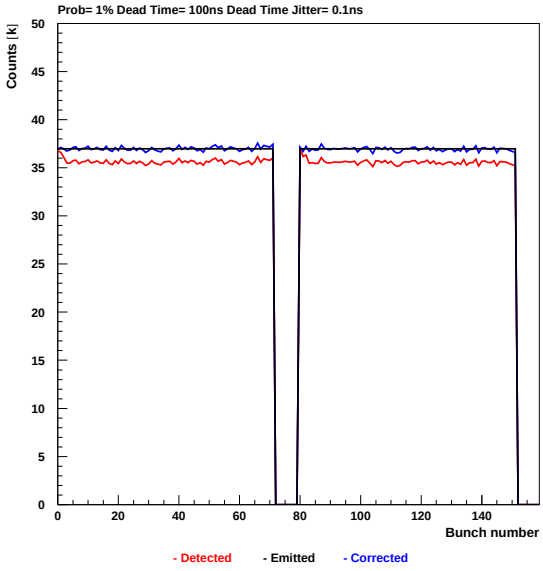

c)

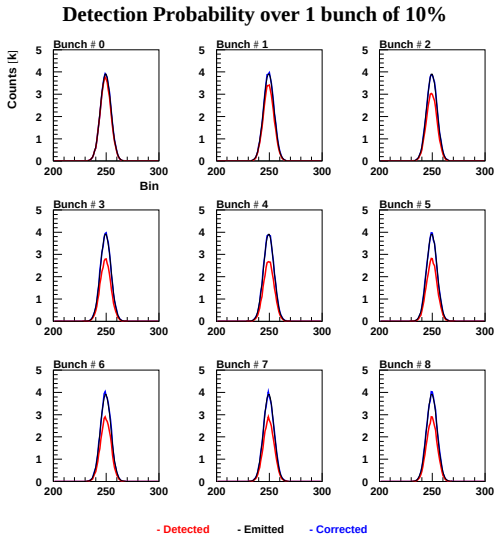

d)

Figure 4: Bunch current distributions for the first two PS batches (see Fig.2 For more explanations) (a)(b)(c). Bunch profiles for the first nine bunches of the ring in the case of 10% emission probability (d). Simulation conditions are; dead time 100ns and dead time jitter 100ps.

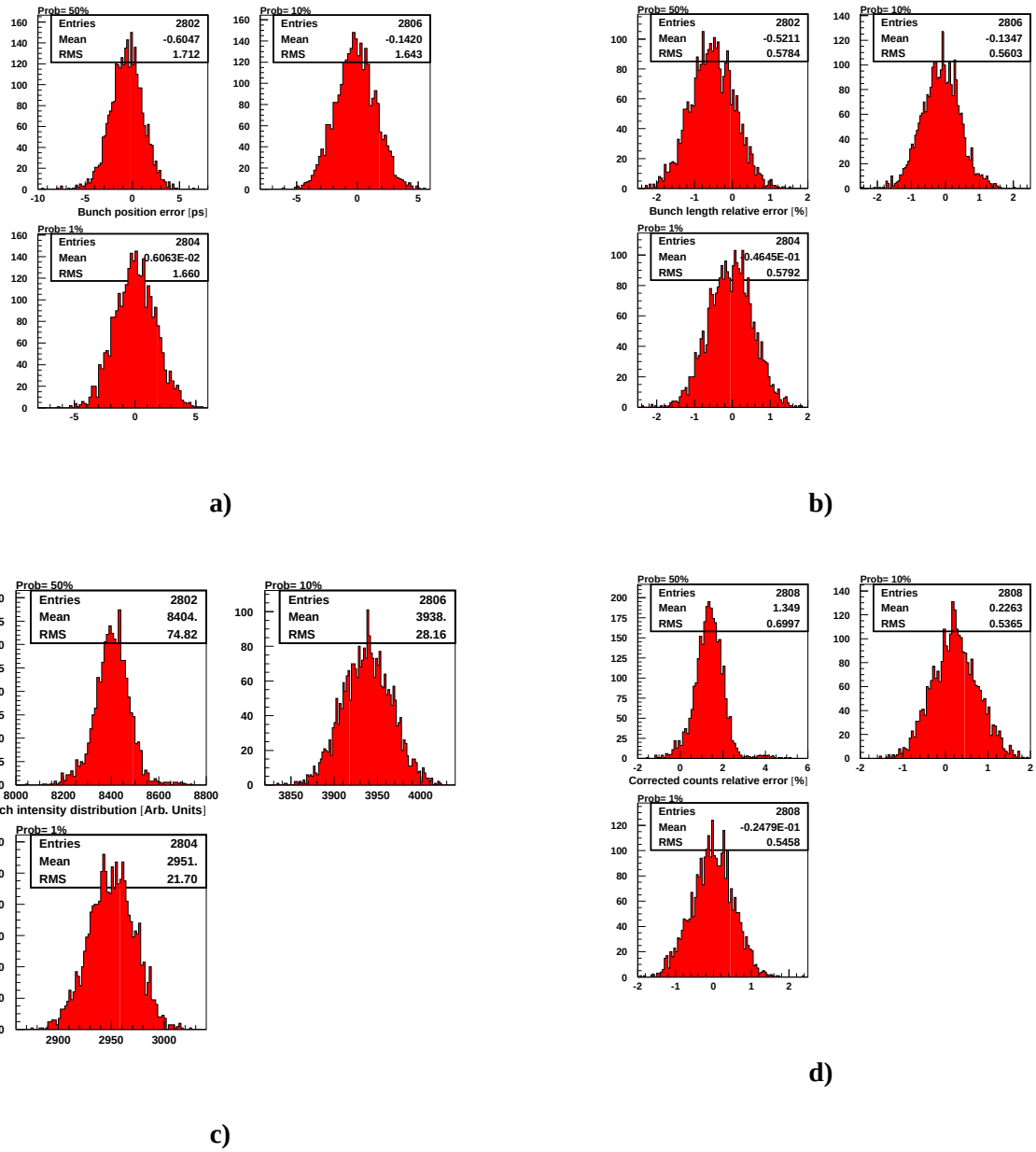

Figure 5: Histograms of the results of the gaussian fits applied to every bunch in the ring (2808.) Bunch position error (a), bunch length error (b), bunch amplitude error (c) and corrected counts vs. emitted photons error (d). Simulation conditions are; dead time 100ns and dead time jitter 100ps.

8.2.2 Dead Time 100ns Jitter 2ns

The results showed in Fig.4 are almost identical to the results obtained for this case and are therefore not repeated.

Fig.6 Shows that even for a much larger dead time jitter the measurement quality is not affected.

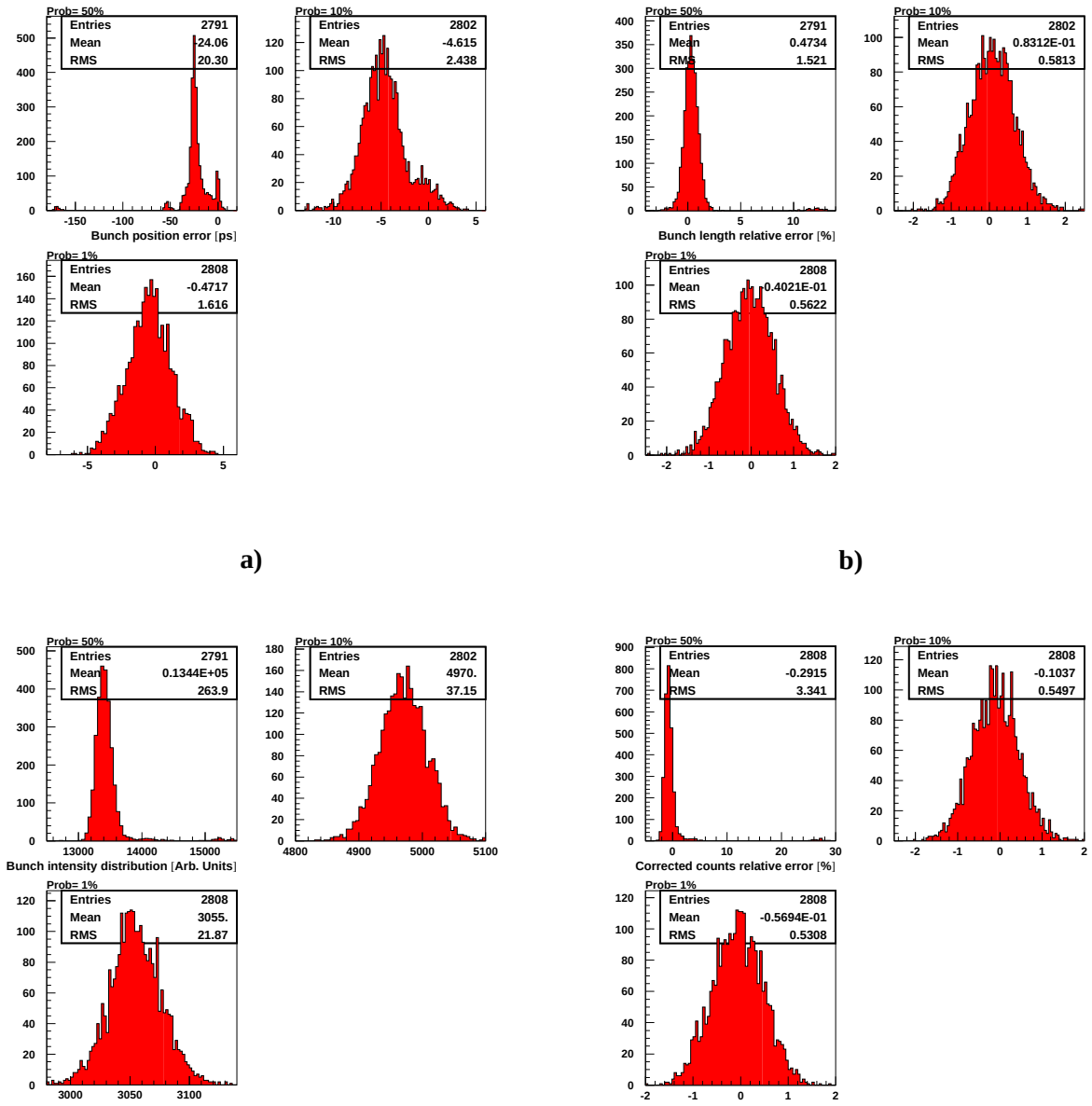

Figure 6: Histograms of the results of the gaussian fits applied to every bunch in the ring (2808.) Bunch position error (a), bunch length error (b), bunch amplitude error (c) and corrected counts vs. emitted photons error (d). Simulation conditions are; dead time 100ns and dead time jitter 2ns.

8.2.3 Dead Time 400ns Jitter 0.1ns

In Fig.7 the case of a dead time larger than the separation between batches is shown. Two important points can be highlighted in this picture. First the dead time has catastrophic effects in case of large emission probabilities, as can also be seen in Fig.8, second there is a carry over effect from batch to batch. At *400ns* there is however still separation between SPS batches since these are separated by 975 *ns*.

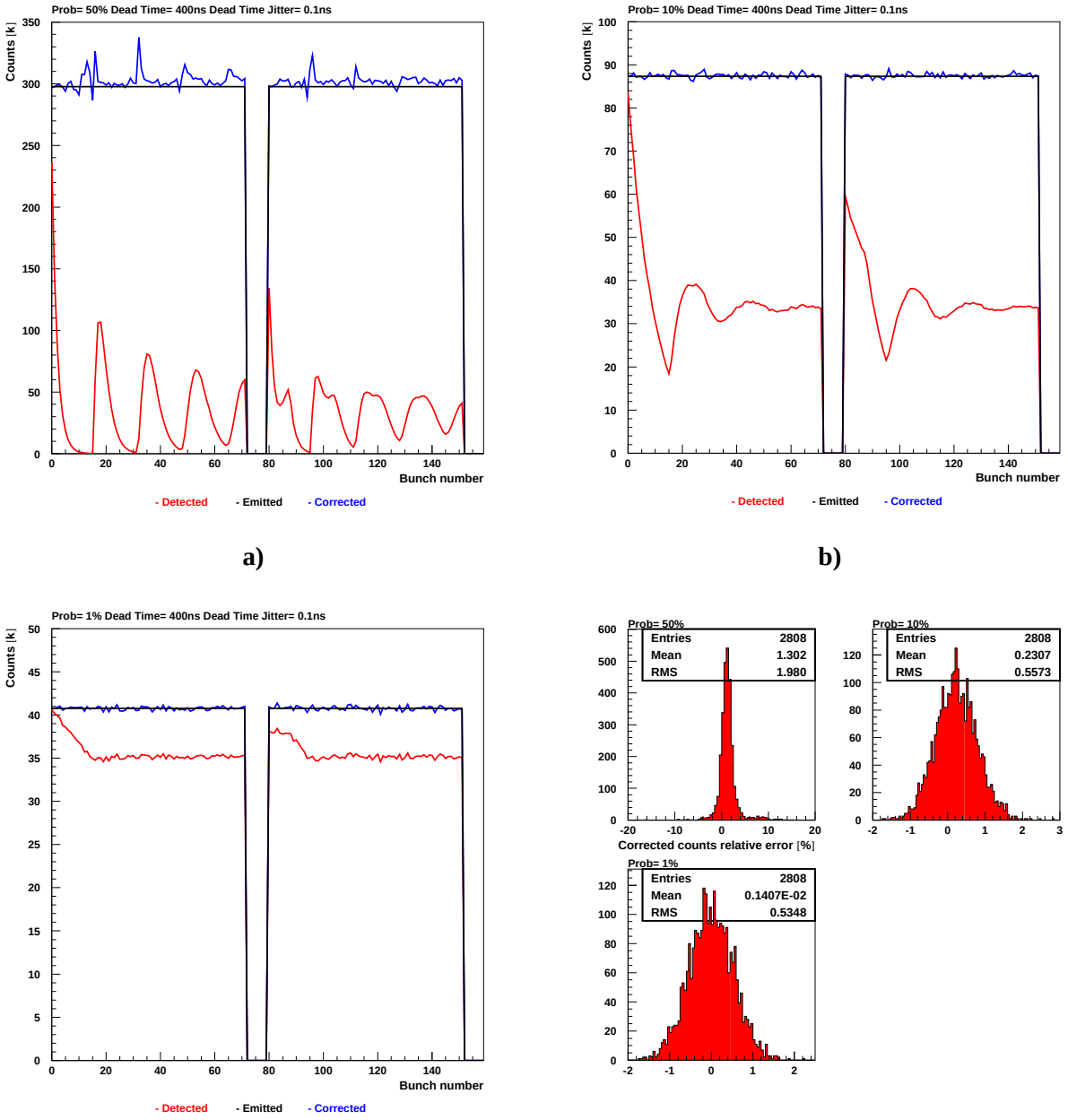

Figure 7: Bunch current distributions for the first two PS batches (see Fig.2 For more explanations) (a)(b)(c). Bunch profiles for the first nine bunches of the ring in the case of 10% emission probability (d). Simulation conditions are; dead time 400ns and dead time jitter 100ps.

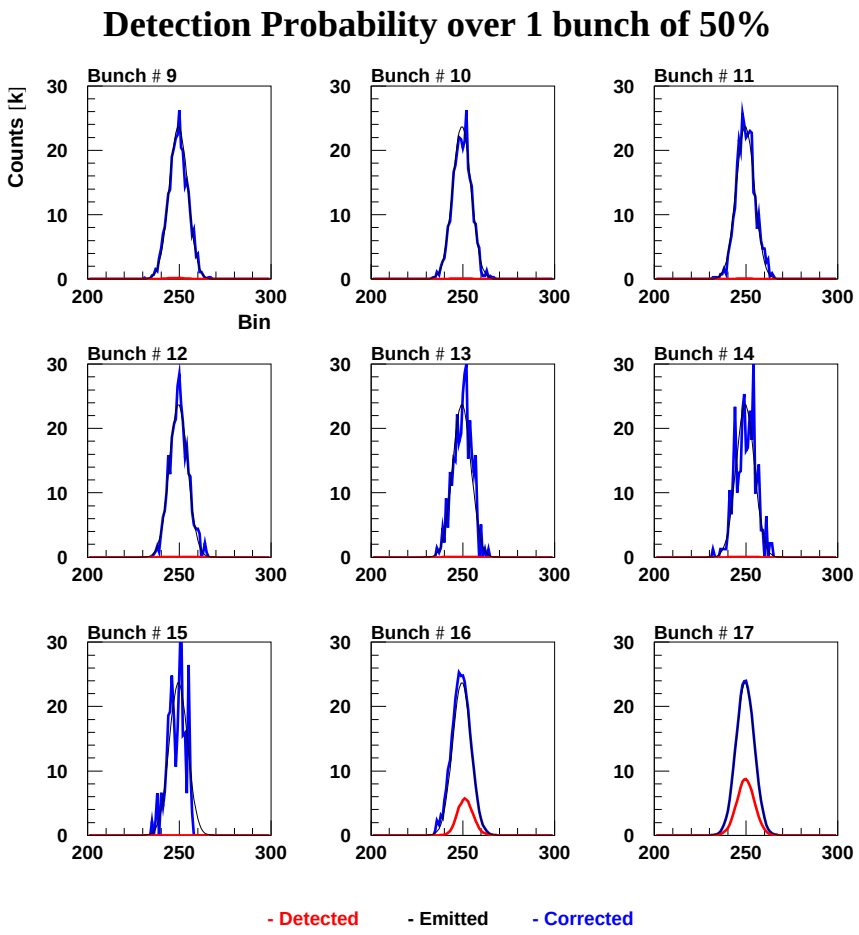

Figure 8 Plot of the profiles of bunches from 9 to 17 of the first PS batch for the case of an emission probability of 50% and dead time of 400ns, dead time jitter is 100ps.

Fig.8 shows the bunch profiles of a few selected bunches for the case of a long dead time (*400 ns*) and a high photon emission rate (*50%*). The signal suppression coming from the shadowing is very important. In some case it is absolutely impossible to see any signal (red curve) at the scale level used in the picture. As a result the error of the corrected profiles (blue curve; dead time corrected counts) is very large.

Fig.9 Shows the measurement errors for the analysed case. It can be seen that even in this case the measurement error is still reasonable. The only difference compared to similar cases but with shorter dead time is the fact that for a larger number of bunches the fitting routine fails to work or gives clearly wrong values, this can be seen by observing the number labelled entries in the plots and comparing this value with the total number of bunches in the machine (2808). Of course by reducing the emission probability this effect can be avoided.

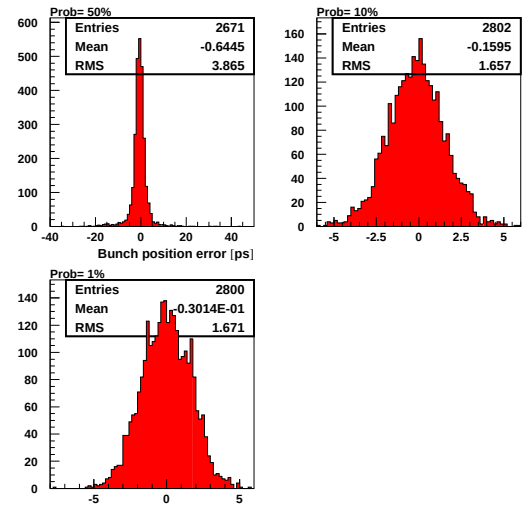

a)

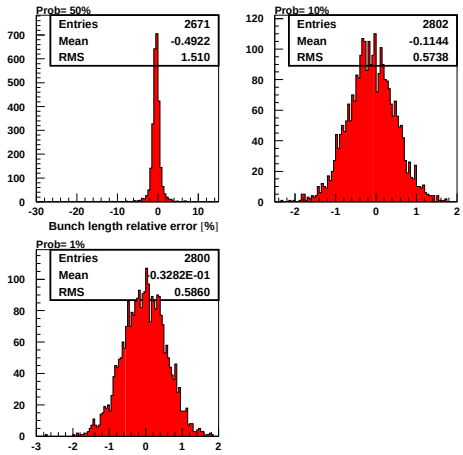

b)

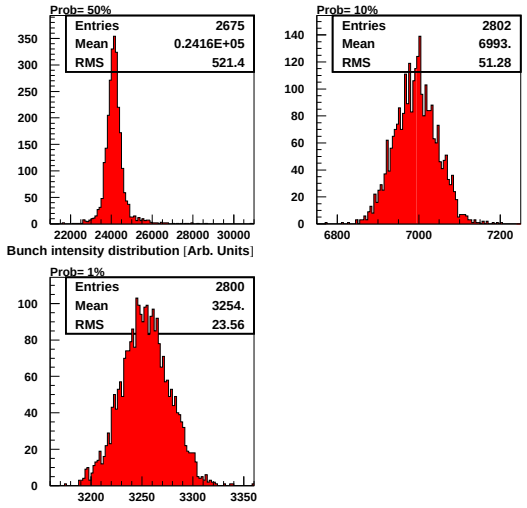

c)

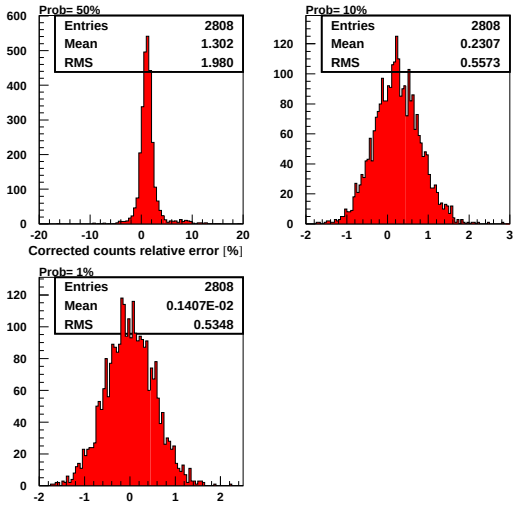

d)

Figure 9: Histograms of the results of the gaussian fits applied to every bunch in the ring (2808.) Bunch position error (a), bunch length error (b), bunch amplitude error (c) and corrected counts vs. emitted photons error (d). Simulation conditions are; dead time 400ns and dead time jitter 100ps.

8.3 Measurement times

It was mentioned that, in the simulation, the number of turns required to generate the desired number of events was recorded. Using this information it is rather easy to calculate the measuring speed of the monitor. The revolution period of LHC is *89 μs*, multiplying the number of turns by the revolution period yields the measurement time. Table 2 shows the values relative to the described simulations. A rough estimation of the time necessary for the detection of one photon can be given by eq. 35. The ratio *3650/2808* accounts for the missing bunches. In order to achieve a bunch length measurement with an error less than *1%* at least *5000* events are necessary per profile[6] (i.e. per bunch), or a total of *14 10⁶* events. This means that for a detector with *100 ns* dead time and an emission probability of *10%*, the measuring time would be of the order of *6* seconds.

$$\Delta t \approx \left(\frac{\tau_b}{S} + \tau_D \right) \cdot \frac{3650}{2808} \tag{35}$$

Dead time	***Emission probability***	***Measurement time for 10^8 events***	***Measurement time for 1 event***	***Measurement time for 14 10^6 (1% error)***
100 ns	50%	18.4 s	184 ns	2.6 s
100 ns	10%	43.8 s	438 ns	6.1 s
100 ns	1%	329 s	3290 ns	46 s
200 ns	50%	30.1 s	301 ns	4.2 s
200 ns	10%	55.4 s	554 ns	7.8 s
200 ns	1%	341 s	3410 ns	48 s
300 ns	50%	41.2 s	412 ns	5.8 s
300 ns	10%	66.7 s	667 ns	9.3 s
300 ns	1%	352 s	3520 ns	49 s
400 ns	50%	53.0 s	530 ns	7.4 s
400 ns	10%	77.7 s	777 ns	11 s
400 ns	1%	363 s	3630 ns	51 s

Table 2 Measurement times for different detection parameters (simulation results).

9 Conclusions

A model for the detection of single photons of synchrotron radiation for the longitudinal density monitors of LHC has been developed. The model has then been used to simulate the system in different conditions. From the results of the simulations it becomes clear that the fact that the proposed photon sensors have an important dead time perturbs heavily the measurement. It was however possible to find a relatively simple correction method that alleviates almost entirely the effects of the dead time, provided that the counting frequency is kept below certain levels.

In conclusion, it was shown that the effects of the dead time must be accounted for in the development of the system, but they do not prevent this technique from being successful.

Another important aspect of the detector: the measurement speed, was also considered. From the values of table 2 it can be seen that the requirements of the specifications document[1] can not be achieved with such a detector. In the mentioned document an accuracy of *1%* of the fit parameters is requested in conjunction with an integration time of *1 ms*. This interval is more that a *1000* times shorter than what present detectors can afford. One possible solution to this problem would be dropping the bunch by bunch measurement and simply average all the *2808* bunches into a single bunch. This would reduce the required integration time by *2808* and thus comply with the request. However the motivations for the short integration time come from synchrotron motion studies and the mentioned averaging could render these studies impossible.

10 References

[1] C. Fischer et al., “HIGH SENSITIVITY MEASUREMENT OF THE LONGITUDINAL DISTRIBUTION OF THE LHC BEAMS”, LHC project document LHC-B-ES-0005.00 rev 2.0, 2003, CERN, Geneva, Switzerland

[2] S. Cova et al, “Evolution and Prospect of Single-Photon Avalanche Diodes and Quenching Circuits”, Single Photon Detector Workshop, NIST, Gaithersburg, MD, USA, March 31- April 1, 2003, http://physics.nist.gov/Divisions/Div844/events/ARDAworkshop/2003/Cova_NIST03.ppt

[3] P. Collier, “Baseline proton filling schemes”, Proc. Chamonix XIII, Chamonix, France, 19 - 23 Jan 2004 - pages 30-33, CERN-AB-2004-014-ADM

[4] O. Brüning et al., “LHC Design Report”, vol.1 the LHC Main Ring, pages 421-422, CERN-2004-003-V-1, 2004, CERN, Geneva, Switzerland

[5] M. Benedikt et al., “LHC Design Report”, vol.3 the LHC Injector Chain, CERN-2004-003-V3, 2004, CERN, Geneva, Switzerland

[6] E. Bravin, “Statistical Effects in Beam Profile Monitors”, CERN-AB-Note-2004-016, 2004, CERN, Geneva, Switzerland